Proton Mobilities in Phosphonic Acid-Based Proton Exchange Membranes Probed by ^{1}H and ^{2}H Solid-State NMR Spectroscopy

Gunther Brunklaus,* Siri Schauff, Dilyana Markova, Markus Klapper, Klaus Müllen, and Hans-Wolfgang Spiess

Max-Planck-Institut für Polymerforschung, Postfach 3148, D-55021 Mainz, Germany

Received: February 24, 2009; Revised Manuscript Received: April 2, 2009

Two novel phosphonic acid-based "dry" proton exchange membrane materials that may allow for fuel cell operation above 100 °C have been prepared and characterized via solid-state ^{1}H and ^{2}H MAS NMR spectroscopy. We obtained information on both the nature of hydrogen bonding and local proton mobilities among phosphonic acid moieties. In particular, ^{2}H MAS NMR line shape analysis yielded apparent activation energies of the underlying motional processes. Using this approach, we have investigated both a model compound and a novel PEM system. It was found that the relation of estimated hydrogen-bond strength and local proton mobility accessible by solid-state NMR and bulk proton conductivity is complex. Improvements through admixture of a second component with protogenic groups are suggested.

I. Introduction

Proton exchange membrane (PEM) fuel cells are referred to as "green batteries" that convert chemical energy of hydrogen and oxygen into electricity and heat, where the electrochemical redox reactions at the electrodes ideally produce water as the only byproduct.[1] Rather long lifetimes and superior energy conversion efficiency render them highly suitable for application in the automotive industry and stationary power systems,[2] while their compactness allows for replacing conventional rechargeable batteries in portable electronic devices.[3,4]

In the past, numerous polymers have been tested as possible materials for PEMs.[5] In particular, sulfonic acid functionalized perfluorinated polymers constitute a class of benchmark compounds that have good mechanical stability and excellent proton conductivities, where Nafion is a frequent representative.[6,7] Despite its wide use, Nafion is limited to moderate operation temperatures ($\leq$80 °C), while low proton conductivity and poor mechanical stability are observed at higher temperatures (>100 °C).[8,9] The exact morphology of Nafion is still under debate, but it appears reasonable to assume a polymer network with channel-like pores that facilitate bulk proton transport.[10,11] Indeed, a more recently introduced rather simple model suggests that the Nafion structure is based on long parallel but otherwise randomly packed water nanochannels surrounded by partially hydrophilic side branches, thus forming inverted-micelle cylinders.[12] Notably, this model cannot only explain important features of Nafion including the fast diffusion of water and protons through Nafion but is also in rather quantitative agreement with experimental small-angle X-ray scattering (SAXS) data of hydrated Nafion.[13] On the basis of an earlier model comprised of periodic cubic arrays of cyclindrical channels, the proton transport mechanism of Nafion was reported as a so-called "vehicle mechanism" that requires a "wet" state of the respective membrane material (e.g., the pores are filled with water), thus allowing a sufficient amount of water molecules to function as a vehicle (e.g., traveling hydronium ions),[14,15] while other studies suggest that the proton conductivity in well-hydrated Nafion is rather dominated by a Grotthus-like hopping mechanism.[16] In all cases, at fixed hydration levels, the bulk proton conductivity was found to decrease with temperature, rendering the long-term high-temperature use of such materials rather difficult even with complicated water management.[17,18] Consequently, many computational efforts are devoted to rationalizing proton conduction mechanisms at low degrees of hydration in sulfonic acid-based polymers.[19,20]

Phosphonic acid functionalized polymers are considered a viable alternative to (per)sulfonated compounds and have been proposed for high-temperature application, since they do not suffer from chemical degradation or detaching effects of the active groups.[19,21] Phosphonic acid units have *two* acidic protons and are both rather amphoteric and less hydrophilic than sulfonic acid, which in principle should allow for a reduced water uptake. Indeed, an uptake of $\approx$1 water molecule per phosphonic acid unit has been found in polyvinyl phosphonic acid[18] compared to at least 4 water molecules in the hydration shell of a sulfonic acid moiety.[22] Hence, a proton transport mechanism rather different from the so-called "vehicle mechanism" has been suggested for phosphonic acids:[14,23] here, protons travel *via* the hydrogen bonds of neighbored phosphonic acid groups (structure diffusion), thus facilitating operation temperatures well above the boiling point of water provided that the PEM material possesses a sufficient thermal stability. This behavior has previously been reported for imidazoles.[20,24] However, most alternative nonperfluorinated PEMs currently have much lower proton conductivities compared to Nafion at similar ion content.[11]

The microstructures of both sulfonated and alternative PEMs are considered to be rather complex, but lacking knowledge of detailed structure−property relationships only permits a trial-and-error strategy in improving the performance of the respective PEM materials. Though the overall fuel cell performance is based on many factors,[9,25] the PEM is the dominating unit. In principle, local proton *mobility* represents a major condition for enabling bulk proton conductivity, and indeed various approaches were already reported to facilitate rather high local proton mobilities.[26] In this work, we explore the so-called spacer concept that simply connects observable proton mobilities (and

* To whom correspondence should be addressed. E-mail: brunklaus@mpip-mainz.mpg.de.

10.1021/jp901714f CCC: $40.75
Published on Web 04/22/2009

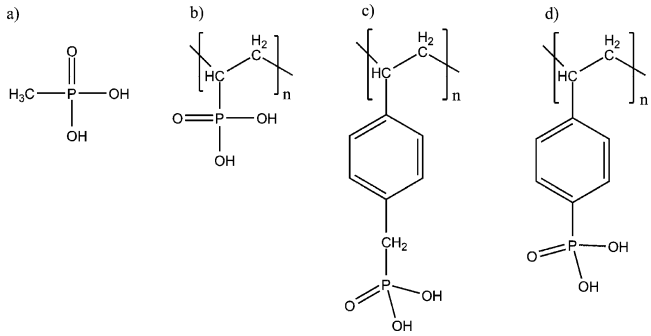

Figure 1. Schematic structures of the considered compounds: (a) MePA; (b) PVPA; (c) PVBzPA; (d) PSPA.

hence bulk conductivities) with the length of a spacer (e.g., an alkyl chain or aromatic moiety) connecting the protogenic group to the polymer backbone. In fact, an increase of the protogenic groups' mobility with increasing spacer length due to the presence of rather dynamic hydrogen bonds allowing for fast bond rupture and formation has been proposed.[14,23] In addition, this concept suggests a critical threshold of the spacer length above which entanglements or possible reactions among the protogenic groups may occur, thus perturbing the dynamic network of hydrogen bonds.

Since structure and dynamics are intimately related concepts in chemistry, it is of utmost importance to identify chemical environments that facilitate high proton mobilities. While it is well-known that proton solvation in both liquids[27] and crystalline solids[28] may yield enhanced proton mobilities, corresponding proton mobilities in rather dry PEM materials are not well understood. Though bulk ionic transport in PEMs is accessible via impedance spectroscopy, it does not provide insight into local proton mobilities. Rather, solid-state NMR under fast magic-angle spinning (MAS) is a powerful and *locally selective* tool for the characterization of functional materials[29] such as PEMs.[30,31]

In this contribution, structural and dynamic properties of both poly(diethyl vinylbenzyl phosphonate) (PVBzPA) and poly(styrene phosphonic acid) (PSPA) are compared to the commercially available model compound methyl phosphonic acid (MePA) and polyvinyl phosphonic acid (PVPA),[31] respectively (cf. Figure 1). PVBzPA and PSPA were chosen as promising candidates for PEM applications, since they combine water insolubility with excellent film forming properties. However, both polymers are *not* available via direct polymerization of the respective phosphonic acid-based monomer but can be prepared via free radical polymerization of the corresponding ester protected monomer followed by hydrolysis, yielding polymers that commonly exhibit very broad molecular weight distributions. The latter commonly indicates the presence of large fractions of oligomers in addition to the desired high-molecular-weight products. The presence of low-molecular-weight fractions, however, may severely affect the bulk properties of the respective material, e.g., proton conductivity or thermal stability, and thus, synthesis of rather well-defined (co)polymers with narrow distributions of molecular weights and low polydispersity is highly desired. In fact, this is most conveniently achieved using the very efficient atom transfer radical polymerization (ATRP) that allows for a variety of architectures.[32] Hence, ATRP was chosen to obtain both poly(diethylvinylbenzyl phosphonate) (PDEVBP) and poly(diethylstyrene phosphonate) (PDESP) that can be converted to the corresponding acid by simple hydrolysis.

II. Methodology

In solid-state ^{1}H NMR, fast MAS is a vital condition to achieve high-resolution spectra of PEM materials.[33] In particular, the ^{1}H chemical shifts of hydrogen-bonded protons are commonly well separated from aliphatic or aromatic protons that may constitute the polymer backbone or side chains of promising PEM materials, and are found at 8−20 ppm, depending on the hydrogen-bond strength.[34] Variable temperature ^{1}H spectra then allow for insights into the respective proton dynamics, as substantial line narrowing is observed in the case of fast motion on the NMR time scale. In addition, mobile protons can be easily distinguished from rather rigid protons applying a homonuclear double-quantum (DQ) filter.[29a] Since observable DQ signals depend on the magnitude of the homonuclear dipolar coupling, missing or reduced proton signal intensities in the respective DQ-filtered spectra indicate averaging of the dipolar couplings, e.g., due to proton dynamics on a time scale faster than the so-called rotor period (at 29762 Hz MAS, $\tau_R = 33.6\ \mu$s). In the case of exchangeable protons (e.g., acidic protons from the protogenic group), site-selective information about dynamic processes taking place in promising PEM materials may be obtained from solid-state ^{2}H NMR spectroscopy.[31,35] Indeed, the quadrupolar tensor of the deuteron is very sensitive to reorientations, as reflected by characteristic changes of the spectral line shapes that not only depend on the dynamic rate but also on the geometry of the underlying motional processes (e.g., exchange among distinct molecular positions) in the nanosecond to second regime. In the case of well-defined molecular motion in an intermediate regime (τ_c around 10−100 μs), the quadrupolar frequency ω_Q is interfering with the molecular correlation time τ_c, causing both severe signal decrease and broadening.[36] Static ^{2}H powder spectra, however, commonly suffer from poor spectral resolution and low sensitivity, while ^{2}H MAS NMR provides substantial gain in the signal-to-noise ratio and improved resolution of chemical species. Under slow MAS, the envelope of the respective spinning sideband pattern reflects the static line shape and in the case of known geometries allows for extraction of dynamic rates (and hence molecular correlation times).[37] Since the width of MAS spinning sidebands is sensitive to exchange broadening, dynamic heterogeneities may be more easily identified under MAS conditions, but generally, motional broadening cannot be undone by MAS.

III. Experimental Section

Samples and Chemicals. All chemicals were obtained from commercial sources and used without further purification unless otherwise noted. The monomer diethyl vinylbenzylphosphonate (DEVBP) was synthesized as described in the literature starting from a vinylbenzyl chloride (mixture containing ∼70% meta- and ∼30% para-isomers).[38] The product of the Arbuzov reaction was purified by flash chromatography on silica, eluting first the unreacted vinylbenzyl chloride with CH_2Cl_2 and then changing to ethyl acetate for the elution of DEVBP. ^{1}H NMR (250 MHz, $CDCl_3$): δ (ppm) 7.33 (2H), 7.21 (2H), 6.66 (1H), 5.7 (1H), 5.2 (1H), 4.22−3.98 (4H), 3.11(2H), 1.26 ppm (6H). ^{13}C NMR (62.5 MHz, $CDCl_3$): δ (ppm) 136.3, 136.1, 130.9, 129.7, 126.17, 113.5, 61.8, 34.4, 32.3, 16.2. ^{31}P NMR (202 MHz, $CDCl_3$): δ (ppm) 25.6.

The monomer diethyl *p*-styrenephosphonate (DESP) was obtained by a palladium-catalyzed phosphonation using the following synthetic protocol: 10 g of 4-bromostyrene (0.055 mol), 8.3 g (0.082 mol) of TEA, and 10.3 g (0.061 mol) of diethyl phosphite were dissolved in 20.5 mL of dry toluene under argon, followed by the addition of 3.156 g (0.0027 mol)

of tetrakis(triphenylphosphine)palladium(0), $Pd[P(Ph)_3]_4$ catalyst under vigorous argon steam. The reaction mixture was slowly heated to 90 °C, and the process was led to proceed at this temperature for 24 h. After cooling, diethyl ether was added to precipitate triethylamine hydrobromide. The precipitate was removed by filtration and the solvents were evaporated to give yellowish viscous oil, which was purified by flash chromatography (ethyl acetate/CH_2Cl_2 solvent system) to give 5.3 g (40.4%) of colorless viscous oil. ^{1}H NMR (250 MHz, CD_2Cl_2): δ (ppm) 7.2−7.6 (4H), 6.55 (1H), 5.67 (1H), 5.15 (1H), 3.98 (4H), 1.22 ppm (6H). ^{13}C NMR (62.5 MHz, CD_2Cl_2): δ (ppm) 141.7, 136.5, 132.5, 129.9, 126.8, 126.5, 116.8, 62.3, 16.6. ^{31}P NMR (202 MHz, $CDCl_3$): δ (ppm) 18.1.

Well-defined polymers from the DEVBP and DESP monomers were prepared via copper-mediated ATRP using α-methylbenzyl bromide as initiator and CuBr in combination with various ligands bearing a different number of coordinating centers to form the catalytic complex, which gives the control over the polymerization. A detailed study on the controlled polymerization of DEVBP via ATRP is discussed elsewhere.[39] For the solid-state NMR studies herein, PDEVBP and PDESP were prepared via ATRP in bulk at 110 °C using the CuBr/*N*,*N*,*N*′,*N*′,*N*″-pentamethyl diethylene triamine (PMDETA) catalytic system. Prior to each ATRP, the polymerization mixtures were carefully degassed by several freeze−pump−thaw cycles and led to polymerize until no further stirring was possible. The obtained polymers were purified by redissolving in a minimum amount of CH_2Cl_2, passing the solutions through a short column filled with neutral Al_2O_3, and dried to a constant weight *in vacuo*. The PDEVBP polymer used in this study had a M_n value of 1.9×10^4 g/mol and a polydispersity index (PDI) of 1.19, while the PDESP exhibited a M_n value of 1.2×10^3 g/mol and a PDI of 1.42.

The molecular weight and the PDI indexes were measured using gel permeation chromatography (GPC). GPC measurements were performed against narrow-dispersed poly(styrene) standards on a Waters device equipped with Styragel columns using dimethylformamide (DMF) as eluent at 60 °C.

The polymeric ethyl phosphonates were converted to the corresponding poly(vinylbenzylphosphonic acid) (PVBzPA) and poly(styrene phosphonic acid) (PSPA) using the bromotrimethylsilane (TMSBr)/methanolysis approach. Typically, the phosphonate was reacted with a 5-fold molar excess of TMSBr relative to the phosphonate groups in CH_2Cl_2 at room temperature for 24 h. After evaporation of the volatiles, the silylated ester was reacted with a large excess of methanol at room temperature for another 24 h. Both PVBzPA and PSPA were obtained in quantitative yields after evaporation of the solvent under reduced pressure and drying in vacuum at room temperature for at least 12 h.

Deuteration. Methyl phosphonic acid (MePA) was deuterated in D_2O, while PVBzPA was dissolved in methanol-d_4 and precipitated. Attempts to deuterate PSPA only yielded poor degrees of deuteration. All compounds were freeze-dried prior to the NMR measurements.

Solid-State NMR Spectroscopy. Most MAS NMR experiments were carried out in 2.5 mm double bearing rotors made from ZrO_2 at spinning rates ranging from 10 to 30 kHz. The ^{1}H and ^{2}H MAS NMR experiments were carried out on a Bruker Avance 700 spectrometer with Larmor frequencies of 700.13 MHz (^{1}H) and 107.474 MHz (^{2}H), respectively. Typical pulse lengths were 2.5 μs for both nuclei. One- and two-dimensional DQ ^{1}H MAS spectra were recorded using the rotor-synchronized back-to-back (BaBa)[40] pulse sequence with excitation and reconversion times of one rotor period (at 29762 Hz MAS, $\tau_R = 33.6$ μs). We applied a nested 16-step phase cycle:[41] for DQ-coherence selection,[42] a four-step phase cycle was applied to the DQ-excitation radio frequency pulse block[43] while the phases of the DQ-reconversion radio frequency pulse block were kept constant. The final reading pulse is then phase-cycled according to the CYCLOPS approach.[44] For the ^{2}H MAS NMR experiments, the magic angle was adjusted at each temperature using dimethylsulfon-d_6. In addition, static ^{2}H NMR spectra were acquired on a Bruker Avance-II 300 MHz spectrometer employing the solid-echo[45] sequence with an interpulse delay of $\tau = 20$ μs and a static probehead (7 mm coil) at 46.072 MHz (^{2}H) with a typical pulse length of 4 μs. In all cases, sample temperatures were calibrated using $Sm_2Sn_2O_7$.[46]

IV. Results and Discussion

Recently, it was reported that methyl phosphonic acid (MePA), integrated in a benzimidazole salt, exhibits fairly high local proton dynamics.[47] The corresponding ^{1}H chemical shift of the acidic protons within the salt was observed at 17 ppm, suggesting rather strong hydrogen bonds. Moreover, the ^{31}P CSA was found to be asymmetric, thus reflecting an inequivalence of the hydrogen bonds involving the protogenic group. In our study, however, methyl phosphonic acid was present as a "free" model compound revealing a rather different behavior. In fact, the static ^{31}P NMR spectrum indicates a symmetric ^{31}P CSA, suggesting an *equivalence* of the hydrogen bonds (cf. the Supporting Information). The ^{1}H MAS spectrum of MePA exhibits two peaks at 1.5 ppm (methyl protons) and 11.3 ppm (acidic protons), respectively, where the latter suggests hydrogen bonds of moderate strength.[48] Since no crystals of MePA suitable for single-crystal X-ray analysis could be obtained, we analyzed the hydrogen-bonding network via 2D ^{1}H−^{1}H double-quantum (DQ) NMR.

In fact, the DQ autocorrelation peak at 22.6 ppm (11.3 ppm + 11.3 ppm) reveals successful formation of a DQ coherence among the acidic protons of the protogenic group (cf. Figure 2b), indicating that these protons are rather immobile (e.g., note the minor reduction of the $PO(OH)_2$ peak intensity in the DQF spectrum (Figure 2a)). In addition, both the autocorrelation peak at 3.0 ppm (1.5 ppm + 1.5 ppm) and the cross-peak at 12.8 ppm (11.3 ppm + 1.5 ppm) confirm the molecular structure of MePA. No significant changes of both the peak line width and the ^{1}H chemical shift of the protogenic group are observed in temperature-dependent ^{1}H MAS NMR spectra of MePA (data not shown), thus suggesting the absence of fast proton dynamics with respect to the NMR time scale, which is indeed consistent with the rather poor bulk proton conductivity of MePA. In contrast to MePA, the acidic protons of PSPA and PVBzPA resonate at 10.8 and 9.2 ppm, respectively. This indicates that the local hydrogen bonding in PSPA is comparable to polyvinyl phosphonic acid (PVPA) (^{1}H chemical shift: 10.8 ppm[31]), while weaker hydrogen bonds are found in PVBzPA. In both cases, the ^{1}H chemical shift of the protogenic group does not change significantly with increasing temperatures, where a noticeable but small splitting of the acidic proton signal in the ^{1}H NMR spectra of PVBzPA at higher temperatures most likely originates from the meta- and para-isomer mixture present in the material. An almost temperature-independent ^{1}H chemical shift suggests that the exchangeable protons populate *equivalent* sites. Indeed, the rather fast proton dynamics (with respect to the NMR time scale) in both PVBzPA and PSPA is nicely reflected by the respective 1D ^{1}H−^{1}H double-quantum-filtered spectra at ambient temperature, where the peak intensity of the $PO(OH)_2$ proton

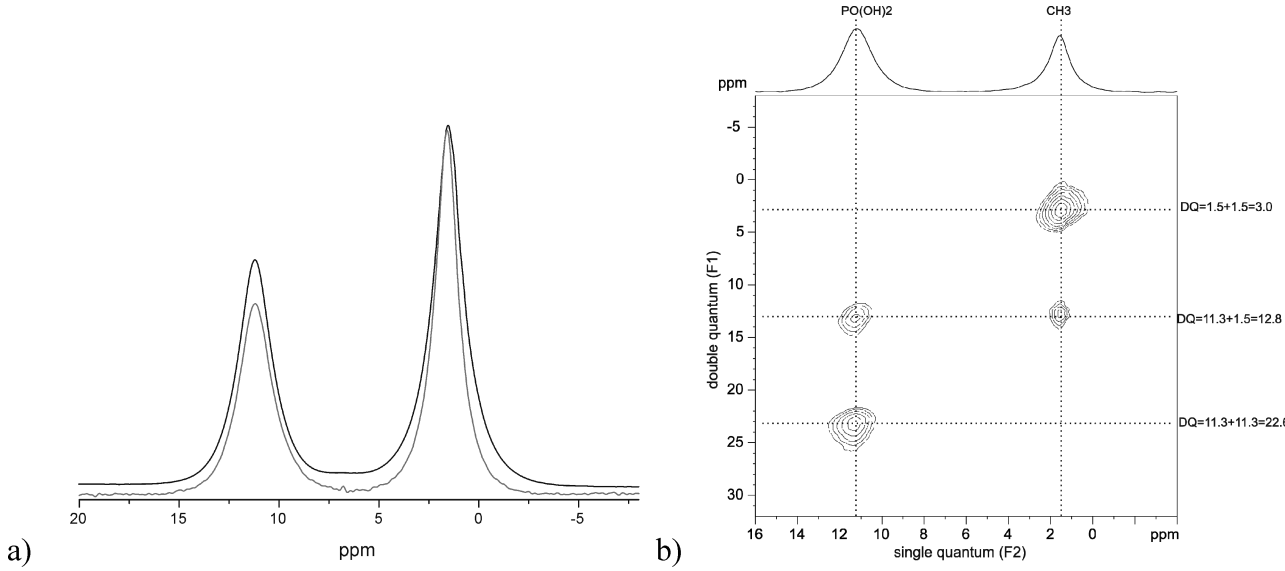

Figure 2. (a) ^{1}H (black) and ^{1}H-DQF ($1t_R$, gray) MAS NMR spectra of MePA recorded at 700.1 MHz and 29762 Hz MAS at ambient temperature (293 K). Note the rather minor reduction of the $PO(OH)_2$ peak intensity in the DQF spectrum. (b) ^{1}H−^{1}H DQ MAS NMR spectrum of MePA at 700.1 MHz and 29762 Hz MAS, acquired under the following experimental conditions: $\tau_{(exc)} = 33.6$ μs, 256 t_1 increments at steps of 33.6 μs, relaxation delay 5 s, 32 transients per increment. Quadrature detection in the F_1-dimension was achieved using the hypercomplex approach (STATES).[49] Eight positive contour levels between 5 and 100% of the maximum peak intensity were plotted. The F_2 projection is shown on the top.

is substantially reduced in comparison to the normal ^{1}H MAS NMR spectra (cf. Figure 3).

The mobility of the protons that reflects the chemical exchange process can be described by a motional correlation time τ_C with respect to the NMR time scale, where either slow or fast exchange comprises the limiting cases. The slow and fast exchange limits are defined by $\tau_C > 10^{-5}$ s and $\tau_C < 10^{-7}$ s, respectively. In the slow exchange limit, the NMR spectrum is a superposition of the resonances arising from each species, while, in the fast exchange limit, a single peak representing an average chemical shift is observed. In this case, the line shape can be described by a Lorentzian with a center frequency of ω and a line width of $\Delta\nu = 1/(\pi T_2^*)$, where T_2^* is the effective transverse relaxation time. Hence, changes in the line widths as a function of temperature can be correlated with an exchange rate Ω, which in the fast exchange limit follows the Arrhenius equation:

$$\Omega = \left(\frac{1}{\Delta\nu}\right) = \Omega_0 \exp\left(-\frac{E_A}{RT}\right) \quad (1)$$

The substantial line narrowing of the $PO(OH)_2$ resonances observed for PSPA and PVBzPA, respectively, clearly reflects rapid exchange motions in the temperature range investigated. In both cases, the line width of the $PO(OH)_2$ resonance reveals a linear dependence on the inverse temperature, thus yielding apparent activation energies of the proton motion of 20 kJ/mol (PSPA) and 16 kJ/mol (PVBzPA), respectively (Figure 4). Though these values are slightly smaller than the apparent activation energy of 25 kJ/mol previously found for PVPA,[31] they fit well with the literature data suggesting (apparent) activation energies of hydrogen bonds in O−H functional groups in the range 20−40 kJ/mol.[13] Notably, the line width and ^{1}H chemical shift of the peak attributed to the aromatic protons of the phenyl ring of both PSPA and PVBzPA do *not* change with increasing temperature, and therefore appear rather rigid and to a first approximation are not involved in the observed acidic proton mobility.

Since the deuteron has a spin of 1, it possesses a quadrupolar moment that can interact with local electric field gradients. The resulting quadrupolar coupling depends on the orientation of the so-called principal axis of the quadrupolar tensor with respect to the magnetic field, so that, under static conditions and in the absence of motion, a well-defined Pake pattern with a quadrupolar splitting ω_Q is obtained. In the presence of motions, however, both the line shape and amplitude of the ^{2}H solid-echo signal are influenced by the geometry and rates of the dynamic processes. When the rate of a well-defined molecular motion becomes comparable to the magnitude of the quadrupolar interaction, the signal intensity is significantly reduced due to destructive interferences during refocusing. This denotes the intermediate motional regime, where a complete loss of the observable ^{2}H NMR signal may occur, as has been experimentally observed in ice where the reorientation of water molecules occurred with a jump rate of 10^5 Hz.[50] In the fast motional regime, the spins experience an averaged interaction, giving rise to powder patterns which depend on the geometry of the motions.

In the case of MePA, at the rather low temperature of 230 K, a Pake pattern with a quadrupolar splitting of about 123 kHz was obtained (cf. Figure 5), which essentially remained unchanged even at elevated temperatures of up to 340 K, thus nicely reflecting the rigidity of the hydrogen-bonding network present in MePA. The ^{2}H MAS NMR spectrum of MePA exhibits a single peak at 11.2 ppm (cf. the Supporting Information) and therefore confirms that the hydrogen-bonding network is unaffected by the deuteration.

Similarly, molecular dynamics can be investigated by temperature-dependent magic-angle spinning (MAS) 1D and 2D ^{2}H NMR experiments. Here, motions lead to characteristic broadening and changes in intensities of the respective spinning sideband pattern. While the exact geometry of the underlying motional processes is difficult to extract from such spinning sideband pattern, signal acquisition under so-called rotor-synchronized conditions (that removes all spinning sidebands) provides superior ^{2}H chemical shift resolution of different sites possibly present in the samples. Since the rotor-synchronized ^{2}H MAS NMR signal also reflects motional broadening (including the signal reduction in the intermediate motional regime),

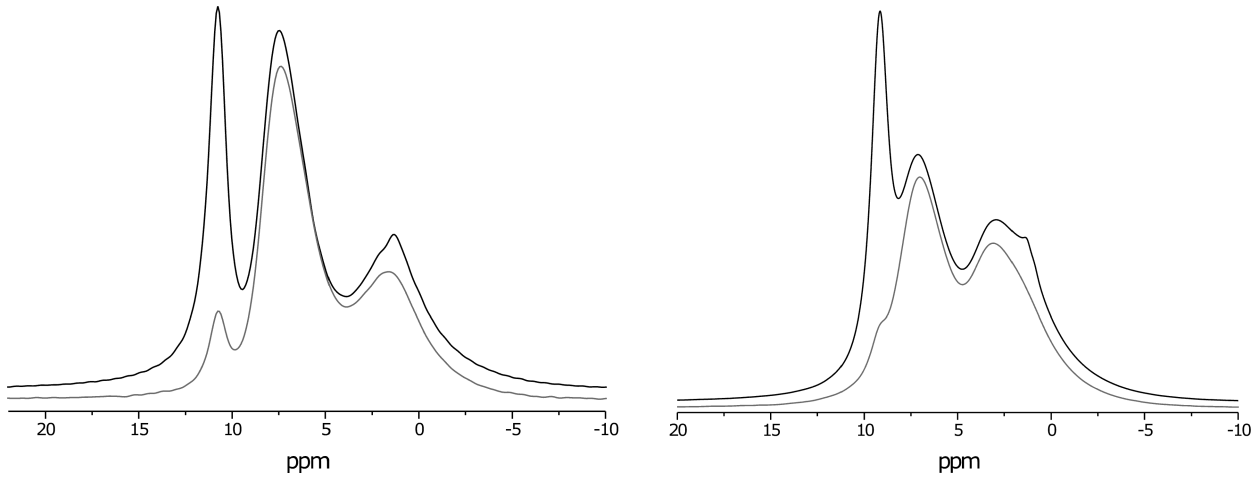

Figure 3. ^{1}H (black) and ^{1}H-DQF ($1t_R$, gray) MAS NMR spectra of PSPA (right) and PVBzPA (left) recorded at 700.1 MHz and 29762 Hz MAS at ambient temperature (293 K). Note the significant reduction of the $PO(OH)_2$ peak intensity in the DQF spectra.

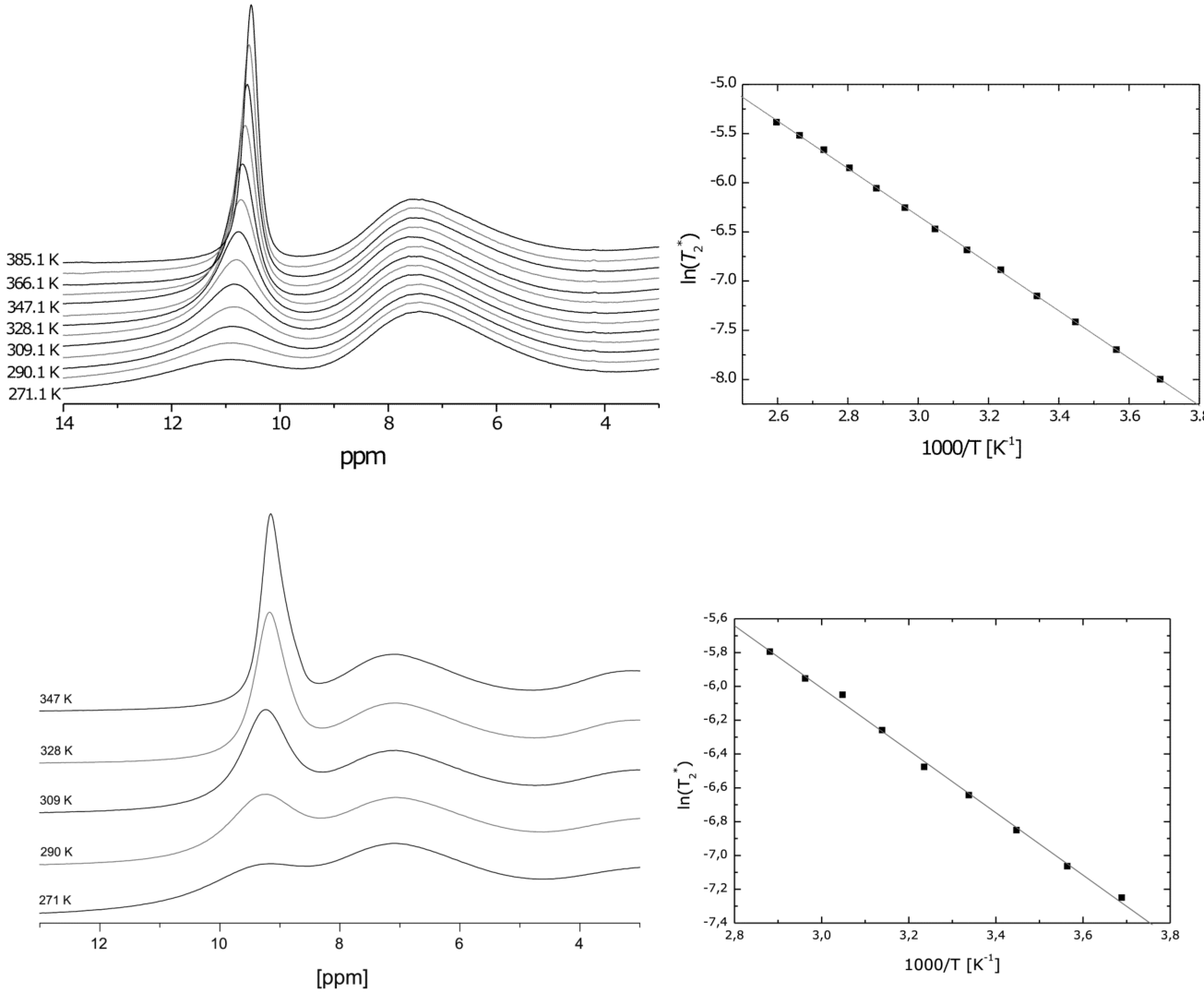

Figure 4. ^{1}H VT MAS spectra and plot of the transverse relaxation time T_2* of the $PO(OH)_2$ peak as a function of temperature, where an Arrhenius-type linear fit of the experimental data is shown for both PSPA (top) and PVBzPA (bottom).

it can be used to qualitatively identify dynamic heterogeneities within the investigated samples, particularly in cases where only a rather low degree of deuteration can be achieved. In the case of dynamic heterogeneities, where either different motional processes (e.g., distinct deuteron sites are involved in different motions) or a distribution of the motional correlation times that are associated with a dynamic process (e.g., some deuterons are faster or slower than others but all are involved in one type of motion) contribute to the observable line broadening, an almost complete reduction of the ^{2}H NMR signal intensities is not very likely.

The corresponding rotor-synchronized ^{2}H MAS NMR spectra of both PVBzPA and PVPA (Figure 6) exhibit a single but fairly

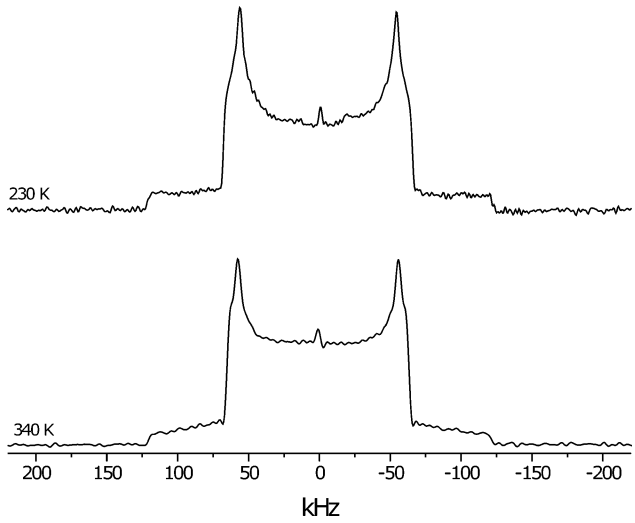

Figure 5. Static ^{2}H spectra of MePA at 230 and 340 K, respectively. Note that the Pake pattern is essentially unaffected by increasing temperatures and indicates an asymmetry parameter of $\eta \approx 0.1$.

broad ^{2}H resonance that reflects the protogenic group ($PO(OD)_2$). In contrast to PVPA, PVBzPA does *not* show an almost complete intensity reduction in the temperature-dependent ^{2}H MAS NMR spectra, which strongly suggests the presence of a rather complex motional process that may be represented by a broad distribution of correlation times. Therefore, activation energies extracted from Arrhenius-type plots have to be considered as *apparent* activation energies, since the experimental ^{2}H MAS NMR line widths may not only reflect contributions from different motional processes but also experience additional line broadening due to mismatch of the magic-angle setting. Nevertheless, these values can be used for comparison of the samples. Apparent activation energies of 38 and 19 kJ/mol were obtained for PVPA[31] and PVBzPA, respectively. Since activation energies of temperature-activated processes in hydrogen bonds can be substantially higher (e.g., up to 120 kJ/mol),[24] the obtained values most probably indicate that the deuteron mobility cannot be attributed to a single, thermally activated process. The spinning sideband ^{2}H NMR spectrum of PVBzPA (Figure 7b) at 295 K has a total width of about 80 kHz, hence indicating a quadrupolar splitting of $\omega_Q = 40$ kHz, which is only $\approx$1/3 of the respective quadrupolar frequencies ω_Q of MePA and PVPA,[31] respectively. This averaging is reminiscent of an axial rotation (e.g., around the C−P bond). The ^{2}H spinning sideband pattern of PVBzPA does not change its shape over temperature, but the center band intensity increases probably due to the residues with the shortest motional correlation times within the distribution. The sideband pattern collapses only when the overall mobility of the sample increases due to (partial) melting, which indicates a rather rigid hydrogen-bonded network in PVBzPA. In contrast, a narrowing of the static ^{2}H line shape at 295 K is observed for PVPA, which at higher temperatures leads to a single sharp peak.[31] Even at low temperatures, a typical Pake pattern could not be observed, indicating general structural differences between PVPA on the one hand and MePA, PVBzPA, and PSPA on the other. Static ^{2}H NMR spectra for PVBzPA and PSPA are not given, since we were not able to receive reasonable signal-to-noise ratios, probably due to the very low degree of deuterons in the acid groups with respect to the polymer backbone.

On the basis of molecular dynamics simulations, however, a reduction of the quadrupolar frequency at elevated temperatures due to a simple jump motion or mere rotation around the C−P bond has been explicitly ruled out for PVPA.[31b] The orientation of the C−P bond with respect to the PVPA backbone was found to remain essentially constant. Rather, a complex proton exchange path along and between the polymer chains that leads to a complete averaging of quadrupolar coupling was proposed. This observation suggests that the connection of the active group ($PO(OH)_2$) to the backbone via a so-called "spacer" has a strong impact on the formation of locally ordered hydrogen-bonded networks, which are flexible yet exhibit mostly local, angular restricted mobility, which is not expected to contribute to proton conduction. For sulfonated siloxanes with a flexible polymer backbone, an increased (water-based) proton conductivity was observed when the alkyl chain length of the spacer was increased.[51] On the other hand, the molecular compound MePA that in a way represents the "simplest" backbone does not reveal any proton mobility (and conductivity) via cooperative rearrangements within a hydrogen-bonded network. In the series PVPA, PSPA, and PVBzPA, however, the measured bulk proton conductivity[39] at about 430 K amounts to 8×10^{-2}, 5×10^{-4},

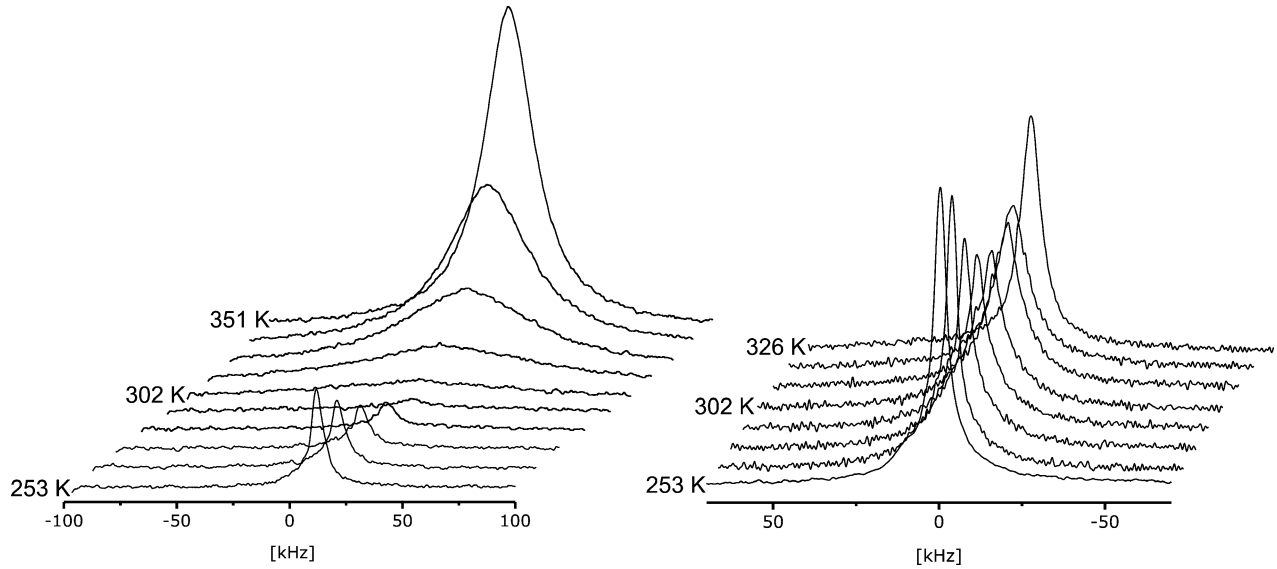

Figure 6. ^{2}H MAS NMR spectra of PVPA (left) and PVBzPA (right) at temperatures ranging from 253 K up to 351 K. Note an almost complete signal loss in the case of PVPA at about 302 K, which is not found for PVBzPA.

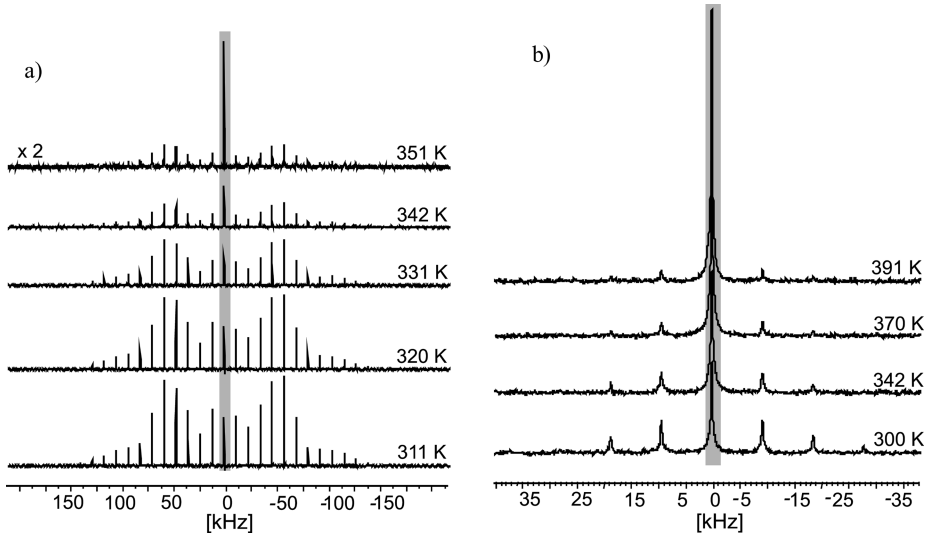

Figure 7. ^{2}H MAS NMR spinning sideband spectra of PVPA (left) and PVBzPA (right) at temperatures ranging from 251 K up to 391 K. The shaded bar indicates the respective center peak.

and 1×10^{-5} S cm^{-1}, respectively, while the apparent activation energies for proton motion are given by 25, 20, and 16 kJ/mol. Since the lowest activation energy is found for PVBzPA, which also shows the lowest bulk proton conductivity and rather weak hydrogen bonds among the $PO(OH)_2$ units, we may conclude that, though the acidic protons are locally mobile, lacking cooperativity of the proton motion within the hydrogen-bonded network does not facilitate sufficient bulk proton transport. Though the hydrogen-bonding strength in PVPA and PSPA is fairly similar (^{1}H chemical shifts of $PO(OH)_2$: 10.6 and 10.8 ppm, respectively), the bulk proton conductivities differ significantly, which again suggests a reduced cooperativity of the proton motion in PSPA compared to PVPA. In the latter case, recent MD simulations revealed that proton motion in polymers can be rather complex. Clearly, there is no simple connection between hydrogen-bonding strength, local mobility, and efficient bulk proton conductivity.

To further explore the influence of possible spacers connecting the protogenic group to the backbone, a series of compounds is currently in preparation in our laboratory. To date, however, there is no routine approach available to predict successful formation of dynamic and cooperative hydrogen-bonding networks based on a given model chemistry that possibly facilitate high proton conductivities, though increasing efforts in modeling of proton conducting materials could be noticed.

V. Conclusion

Poly(diethylvinylbenzyl phosphonate) and poly(diethylstyrene phosphonate) were obtained from copper-mediated ATRP, and quantitatively converted to the corresponding phosphonic acid via TMSBr/methanolysis under mild conditions. Solid-state ^{1}H and ^{2}H NMR experiments have been successfully applied to gain information on the nature of the hydrogen-bonded network and respective proton and/or deuteron mobilities in PVPA, PSPA, and PVBzPA, respectively. It was found that the so-called "spacer" that connects the protogenic group ($PO(OH)_2$) to the polymer backbone has a strong impact on the formation of locally ordered hydrogen-bonded networks, which exhibit local angular restricted proton mobility. Though the acidic protons can be locally mobile, lacking cooperativity of the proton motion within the network does not facilitate sufficient bulk proton transport. Clearly, there is no simple connection between hydrogen-bonding strength, local mobility, and efficient bulk proton conductivity.

While rather anhydrous proton conducting materials based on structural diffusion have shown poor to moderate bulk proton conductivities, water- or solvent-based ("vehicular") systems revealed excellent proton conductivities but may suffer from solvent leaching.[52] This suggests that a combination of the two approaches, that is, an amphoteric protogenic group immobilized in a stabilizing matrix supported by a nonleaching "vehicle" (e.g., small oligomers that may also carry a protogenic group), could be rather beneficial in achieving higher conductivities. Further work along this line is in progress.

Acknowledgment. The authors thank Dr. Lothar Brombacher and Dr. Christoph Deller for fruitful discussions and Verona Maus, Manfred Hehn, and Hans-Peter Raich for technical support. Financial support, provided by the grant BMBF GIN-SF-049, is gratefully acknowledged.

Supporting Information Available: The static ^{31}P NMR and ^{2}H MAS NMR spectra of MePA. This material is available free of charge via the Internet at http://pubs.acs.org.

References and Notes

(1) Sopian, K.; Wan Daud, W. R. *Renewable Energy* **2006**, *31*, 719–727.
(2) Du, B.; Guo, Q.; Pollard, R.; Rodriguez, D.; Smith, C.; Elter, J. *JOM* **2006**, 45–49.
(3) Steele, B. C. H.; Heinzel, A. *Nature (London)* **2001**, *414*, 345–352.
(4) Winter, M.; Brodd, R. J. *Chem. Rev.* **2004**, *104*, 4245–4269.
(5) (a) Hickner, M. A.; Ghassemi, H.; Kim, Y. S.; Einsla, B. R.; McGrath, J. E. *Chem. Rev.* **2004**, *104*, 4587–4612. (b) Rikukawa, M.; Sanui, K. *Prog. Polym. Sci.* **2000**, *25*, 1463–1502. (c) Kerres, J. A. *J. Membr. Sci.* **2001**, *185*, 47–66.
(6) Carrette, L.; Friedrich, K. A.; Stimming, U. *Fuel Cells* **2001**, *1*, 5–39.
(7) Kundu, P. P.; Pal, A. *Rev. Chem. Eng.* **2006**, *22*, 125–153.
(8) Kim, E.; Weck, P. F.; Balakrishnan, N.; Bae, C. *J. Phys. Chem. B* **2008**, *112*, 3283–3286.
(9) Shao, Y.; Yin, G.; Wang, Z.; Gao, Y. *J. Power Sources* **2007**, *167*, 235–242.
(10) Munowitz, K. A.; Moore, R. B. *Chem. Rev.* **2004**, *104*, 4535–4585.
(11) Gebel, G.; Diat, O. *Fuel Cells* **2005**, *5*, 261–276.
(12) Schmidt-Rohr, K.; Chen, Q. *Nat. Mater.* **2008**, *7*, 75–83.
(13) (a) Rubatat, L.; Rollet, A. L.; Gebel, G.; Diat, O. *Macromolecules* **2002**, *35*, 4050–4055. (b) Rubatat, L.; Gebel, G.; Diat, O. *Macromolecules* **2004**, *37*, 7772–7783.

(14) Kreuer, K. D.; Paddison, S. J.; Spohr, E.; Schuster, M. *Chem. Rev.* **2004**, *104*, 4637–4678.
(15) Ye, G.; Janzen, N.; Goward, G. R. *Macromolecules* **2006**, *39*, 3283–3290.
(16) Thompson, E. L.; Capehart, T. W.; Fuller, T. J.; Jorne, J. *J. Electrochem. Soc.* **2006**, *153*, A2351–A2362.
(17) Smitha, B.; Sridhar, S.; Khan, A. A. *J. Membr. Sci.* **2005**, *259*, 10–26.
(18) Kaltbeitzel, A.; Schauff, S.; Steininger, H.; Bingöl, B.; Brunklaus, G.; Meyer, W. H.; Spiess, H. W. *Solid State Ionics* **2007**, *178*, 469–474.
(19) (a) Paddison, S. J.; Elliot, J. A. *J. Phys. Chem. A* **2005**, *109*, 7583–7593. (b) Paddison, S. J.; Kreuer, K. D.; Maier, J. *Phys. Chem. Chem. Phys.* **2006**, *8*, 4530–4542. (c) Elliot, J. A.; Paddison, S. J. *Phys. Chem. Chem. Phys.* **2007**, *9*, 2602–2618.
(20) Cui, S.; Liu, J.; Selvan, M. E.; Keffler, D. J.; Edwards, B. J.; Steele, W. V. *J. Phys. Chem. B* **2007**, *111*, 2208–2218.
(21) (a) Schuster, M.; Rager, T.; Noda, A.; Kreuer, K. D.; Maier, J. *Fuel Cells* **2005**, *5*, 355–365. (b) Miyatake, K.; Hay, A. S. *J. Polym. Sci., Part A: Polym. Chem.* **2001**, *39*, 3770–3779. (c) Meng, Y. Z.; Tjong, S. C.; Hay, A. S.; Wang, S. J. *Eur. Polym. J.* **2003**, *39*, 627–631.
(22) Mologin, D. A.; Khalatur, P. G.; Khokhlov, A. R. *Macromol. Theory Simul.* **2002**, *11*, 587–607.
(23) Kreuer, K. D. *Chem. Mater.* **1996**, *8*, 610–641.
(24) Goward, G. R.; Schuster, M. F. H.; Sebastiani, D.; Schnell, I.; Spiess, H. W. *J. Phys. Chem. B* **2002**, *106*, 9322–9334.
(25) Vishnyakov, V. M. *Vacuum* **2006**, *80*, 1053–1065.
(26) (a) Steininger, H.; Schuster, M.; Kreuer, K. D.; Kaltbeitzel, A.; Bingöl, B.; Meyer, W. H.; Schauff, S.; Brunklaus, G.; Maier, J.; Spiess, H. W. *Phys. Chem. Chem. Phys.* **2007**, *9*, 1764–1773. (b) Ioselevich, A. S.; Kornyshev, A. A.; Steinke, J. H. G. *J. Phys. Chem. B* **2004**, *108*, 11953–11963. (c) Peckham, T. J.; Schmeisser, J.; Holdcroft, S. *J. Phys. Chem. B* **2008**, *112*, 2848–2858. (d) Cánovas, M. J.; Sobrados, I.; Sanz, J.; Acosta, J. L.; Linares, A. *J. Membr. Sci.* **2006**, *280*, 461–469. (e) Tsang, E. M. W.; Zhang, Z.; Shi, Z.; Soboleva, T.; Holdcroft, S. *J. Am. Chem. Soc.* **2007**, *129*, 15106–15607. (f) Schuster, M. F. H.; Meyer, W. H. *Annu. Rev. Mater. Res.* **2003**, *33*, 233–261.
(27) Agmon, N. *Isr. J. Chem.* **1999**, *39*, 493–502.
(28) Potier, A. *J. Solid State Mater.* **1992**, *2*, 1–17.
(29) (a) Brown, S. P.; Spiess, H. W. *Chem. Rev.* **2001**, *101*, 4125–4155. (b) Reichert, D. *Annu. Rep. NMR Spectrosc.* **2005**, *55*, 159–203. (c) Eckert, H.; Elbers, S.; Epping, J. D.; Janssen, M.; Kalwei, M.; Strojek, W.; Voigt, U. *Top. Curr. Chem.* **2005**, *246*, 195–233. (d) Ashbrook, S. E.; Smith, M. E. *Chem. Soc. Rev.* **2006**, *35*, 718–735. (e) Brown, S. P. *Prog. Nucl. Magn. Reson.* **2007**, *50*, 199–251. (f) Harris, R. K. *Solid State Sci.* **2004**, *6*, 1025–1037. (g) Taulelle, F. *Solid State Sci.* **2004**, *6*, 1053–1057. (h) Harris, R. K. *Analyst* **2006**, *131*, 351–373.
(30) (a) Celik, S. U.; Akbey, U.; Bozkurt, A.; Graf, R.; Spiess, H. W. *Macromol. Chem. Phys.* **2008**, *209*, 593–603. (b) Celik, S. U.; Akbey, U.; Graf, R.; Bozkurt, A.; Spiess, H. W. *Phys. Chem. Chem. Phys.* **2008**, *10*, 6058–6066. (c) Vijayakumar, M.; Traer, J. W.; Britten, J. F.; Goward, G. R. *J. Phys. Chem. C* **2008**, *112*, 5221–5231. (d) Ye, G.; Fortier-McGill, B.; Traer, J. W.; Czardybon, A.; Goward, G. R. *Macromol. Chem. Phys.* **2007**, *208*, 2076–2084.
(31) (a) Lee, Y. J.; Bingöl, B.; Murakhtina, T.; Sebastiani, D.; Meyer, W. H.; Wegner, G.; Spiess, H. W. *J. Phys. Chem. B* **2007**, *111*, 9711–9721. (b) Lee, Y. J.; Murakhtina, T.; Sebastiani, D.; Spiess, H. W. *J. Am. Chem. Soc.* **2007**, *129*, 12406–12407.
(32) Patten, E.; Matyjaszewski, K. *Adv. Mater.* **1998**, *10*, 901–915.
(33) Traer, J. W.; Montoneri, E.; Samoson, A.; Past, J.; Tuherm, T.; Goward, G. R. *Chem. Mater.* **2006**, *18*, 4747–4754.
(34) Becker, E. D. Hydrogen Bonding. In *Encyclopedia NMR*; Grant, D. M., Harris, R. K., Eds.; 1996; Vol. 4, pp 2415−2420.
(35) Spiess, H. W. *Adv. Polym. Sci.* **1985**, *66*, 24–56.
(36) Cutajar, M.; Ashbrook, S. E.; Wimperis, S. *Chem. Phys. Lett.* **2006**, *423*, 276–281.
(37) Hologne, M.; Hirschinger, J. *Solid State Nucl. Magn. Reson.* **2004**, *26*, 1–10.
(38) Yu, Z.; Zhu, W. X.; Cabasso, I. *J. Polym. Sci., Part A: Polym. Chem.* **1990**, *28*, 227–230.
(39) Markova, D.; Kumar, A.; Klapper, M.; Müllen, K. Submitted for publication.
(40) (a) Geen, H.; Titman, J. J.; Gottwald, J.; Spiess, H. W. *Chem. Phys. Lett.* **1994**, *227*, 79–86. (b) Gottwald, J.; Demco, D. E.; Graf, R.; Spiess, H. W. *Chem. Phys. Lett.* **1995**, *243*, 314–323.
(41) Zuckerstätter, G.; Müller, N. *Concepts Magn. Reson., Part A* **2007**, *30*, 81–99.
(42) (a) Bodenhausen, G.; Kogler, H.; Ernst, R. R. *J. Magn. Reson.* **1984**, *58*, 370–388. (b) Bain, A. D. *J. Magn. Reson.* **1984**, *56*, 418–427.
(43) Levitt, M. H.; Madhu, P. K.; Hughes, C. E. *J. Magn. Reson.* **2002**, *155*, 300–306.
(44) Hoult, D. I.; Richards, R. E. *Proc. R. Soc. London, Ser. A* **1975**, *344*, 311–340.
(45) Furó, I.; Hedin, N. *J. Magn. Reson.* **2001**, *152*, 214–216.
(46) Langer, B.; Schnell, I.; Spiess, H. W.; Grimmer, A. R. *J. Magn. Reson.* **1999**, *138*, 182–186.
(47) Traer, J. W.; Britten, J. F.; Goward, G. R. *J. Phys. Chem. B* **2007**, *111*, 5602–5609.
(48) Chierotti, R. M.; Gobetto, R. *Chem. Commun.* **2008**, *14*, 1621–1634.
(49) States, D. J.; Haberkorn, R. A.; Ruben, D. J. *J. Magn. Reson.* **1982**, *48*, 286–292.
(50) Wittebort, R. J.; Usha, M. G.; Ruben, D. J.; Wemmer, D. E.; Pines, A. *J. Am. Chem. Soc.* **1988**, *110*, 5668–5671.
(51) Steininger, H.; Schuster, M.; Kreuer, K. D. *Solid State Ionics* **2006**, *177*, 2457–2462.
(52) A de Bruijn, F.; Makkus, C. R.; Mallant, R. K. A. M.; Janssen, G. J. M. *Adv. Fuel Cells* **2007**, *1*, 235–336.

JP901714F